

**Saturation and electron-beam lifetime in a storage ring free-electron laser**R. Bartolini,<sup>1</sup> G. Dattoli,<sup>1</sup> L. Giannessi,<sup>1</sup> L. Mezi,<sup>1</sup> A. Renieri,<sup>1</sup> M. Migliorati,<sup>2</sup> C. Bruni,<sup>3,4</sup> M. E. Couprie,<sup>3,4</sup> D. Garzella,<sup>3,4</sup> and G. Orlandi<sup>3,4</sup><sup>1</sup>*ENEA, Unità Tecnico Scientifica Tecnologie Fisiche Avanzate, Centro Ricerche Frascati, Casella Postale, 65-00044 Frascati, Rome, Italy*<sup>2</sup>*Dipartimento di Energetica, Università di Roma, La Sapienza, Rome, Italy*<sup>3</sup>*CEA, Service de Photons, Atomes, et Molécules, Bâtiment 522, 91 191 Gif-sur-Yvette, France*<sup>4</sup>*LURE, Université Paris-Sud, Bâtiment 209D, 91 898 Boîte Postale 34, Paris, France*

(Received 23 May 2003; published 4 March 2004)

We present a phenomenological treatment of free-electron laser storage ring saturation dynamics. The model includes longitudinal instabilities, Touschek intrabeam scattering, and nonzero off-energy-function contributions. The model predictions are compared with Super ACO experimental results and the agreement is shown to be satisfactory.

DOI: 10.1103/PhysRevE.69.036501

PACS number(s): 29.20.Dh, 42.55.Tv

**I. INTRODUCTION**

The free-electron laser (FEL) dynamics in storage ring (SR) accelerators is a complex phenomenon, with implications going well beyond the simple generation of coherent radiation [1]. The dynamics of the whole system should be considered from a unitary point of view, and the FEL should be viewed as one of the intrinsic feedback mechanisms contributing to the electron-beam equilibrium with the accelerator environment. A self-consistency loop accounting for the previous statement is shown in Fig. 1, where we have reported the interplay of the coupled electron-beam–FEL “system.” By assuming that the system has initially reached a kind of equilibrium, the onset of the FEL induces a beam heating which provides different conditions for the dynamics of the longitudinal instabilities of microwave and sawtooth type [1–3], which are also responsible for beam heating. The FEL and longitudinal instabilities may in turn modify other mechanisms like the Touschek intrabeam scattering (TIS) [4] and the head-tail instability [5]. These combined effects provide a variation of the electron-beam characteristics, which in turn affect the FEL dynamics until saturation occurs.

The arrow external to the loop accounts for a long term effect concerning the Touschek lifetime [4], and occurring on a time scale (hours) much larger than the FEL dynamics characteristic times, namely, the laser rise time (microsecond range) and damping time (millisecond range).

The main assumption underlying the previous analysis [1] is essentially that the FEL produces beam heating [6], which combines with that provided by the natural synchrotron radiation emission [7], thus determining the conditions for the evolution of transverse or longitudinal instabilities and of the other previously mentioned effects.

Equilibrium conditions are achieved once the FEL has reached saturation. The mechanisms leading to saturation are complex too; they do not reflect only the effect of the cumulative induced energy spread, but also the contributions from the instabilities, from multiple Touschek scattering, and so on. Furthermore, any contribution leading to a gain reduction may be a source of FEL saturation, such as, e.g., a poor

overlapping between electron beam and laser beam, due to an increase of the electron-beam transverse dimensions associated with a nonzero dispersion function inside the FEL undulator [8]. In this case the FEL induced energy spread determines, along with the increase of the longitudinal beam dimension, an increase of its transverse size also in the interaction region.

One of the macroscopic consequences of the FEL saturation is therefore an increase of the electron-bunch volume, which implies an increase of the electron-beam lifetime, also. Here we will show that this last effect has been experimentally observed and we will see that the relevant results can be quantitatively explained. We will also discuss how the model of FEL–electron-beam interaction introduced in [1] and references therein can be further implemented, and how the underlying dynamics provides further enlightening insight into the noise-nonlinearity interplay discussed in Ref. [1].

**II. DYNAMICAL EQUATIONS**

In this section we will discuss how TIS, instability of the sawtooth type (STI) [9], and FEL dynamics can be merged within the framework of a unified description. To make the problem more understandable and to better clarify its physical implications, we will proceed in gradual steps, by describing separately the various elements of the game.

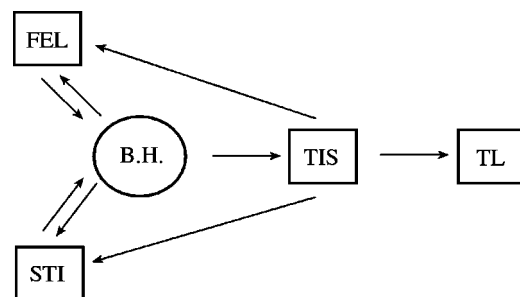


FIG. 1. Loop diagram of dynamical effect in SR-FEL dynamics: beam heating (BH), FEL, sawtooth instability (STI), Touschek intrabeam scattering (TIS), Touschek lifetime (TL).

### A. STI-TIS interplay

The model equations accounting for the dynamics of STI [10] are reported below:

$$\begin{aligned} \frac{d}{dt} \sigma_i^2 &= \left( \alpha - \frac{2}{\tau_s} \right) \sigma_i^2, \\ \frac{d}{dt} \alpha &= \left[ \frac{A}{(1 + \sigma_i^2)^{1/4}} - B(1 + \sigma_i^2)^{1/2} \right], \end{aligned} \quad (1)$$

$$A = \frac{n}{T} \sqrt{\frac{(2\pi)^{3/2} I_0 \nu_s |Z_n/n|}{E_0/e\sigma_{\varepsilon,n}}}, \quad B = \frac{2\pi n}{T} \alpha_c \sigma_{\varepsilon,n},$$

where  $\sigma_i$  denotes the ratio of the energy spread induced by the instability to the natural energy spread  $\sigma_{\varepsilon,n}$ ,  $T$  is the machine revolution period,  $E_0$  the nominal energy,  $e$  the electron charge,  $I_0$  the average current,  $\alpha_c$  the momentum compaction,  $n$  a harmonic of the revolution frequency,  $|Z_n/n|$  the machine impedance, and  $\nu_s$  the synchrotron tune.

The instability growth rate is controlled by  $\alpha$ , and the second of Eqs. (1) states that its evolution is due to a perturbation induced by the wake field and counteracted by the Landau damping, associated with the spread in oscillation frequencies [10]. By following Ref. [11] we write the solution of the first of Eqs. (1) in the form

$$\begin{aligned} \sigma_i^2(t) &= \exp \left[ g(t, \sigma_{i,0}, \alpha_0) - 2 \frac{t}{\tau_s} \right], \\ g(t, \sigma_{i,0}, \alpha_0) &= \int_0^t \alpha(t', \sigma_{i,0}, \alpha_0) dt' \end{aligned} \quad (2)$$

with  $\sigma_{i,0}$  and  $\alpha_0$  denoting the initial conditions of Eqs. (1).

In Fig. 2 we report the functions  $g$ ,  $2t/\tau_s$ , and  $\alpha$ . It is evident that the function  $g$  has a steplike behavior with an average slope  $2/\tau_s$ . Corresponding to any step there is a sharp increase and decrease of  $\alpha$ . Any mechanism capable of bringing the average slope of  $g$  below  $2/\tau_s$  will determine the switching off of the instability (see Ref. [11] for further comments).

The TIS is due to Coulomb scattering and its most significant manifestation is an increase of the induced energy spread, according to the relation [4]

$$\sigma^2(\sigma^2 + 1)^2 = Rf \left( \frac{S}{(\sigma^2 + 1)^{3/2}} \right), \quad (3)$$

$$f(\xi) = \int_{\xi}^{\infty} \frac{1}{x} e^{-x} \ln x \, dx,$$

where  $\sigma$  denotes the ratio of the induced energy spread to the natural part and  $R$  and  $S$  are constants depending on the specific machine parameters. The inclusion of these effects is accomplished by modifying Eqs. (3) and the second of Eqs. (1) as follows:

$$\sigma^2(\sigma^2 + \sigma_i^2 + 1)^2 = Rf \left( \frac{S}{(\sigma^2 + \sigma_i^2 + 1)^{3/2}} \right),$$

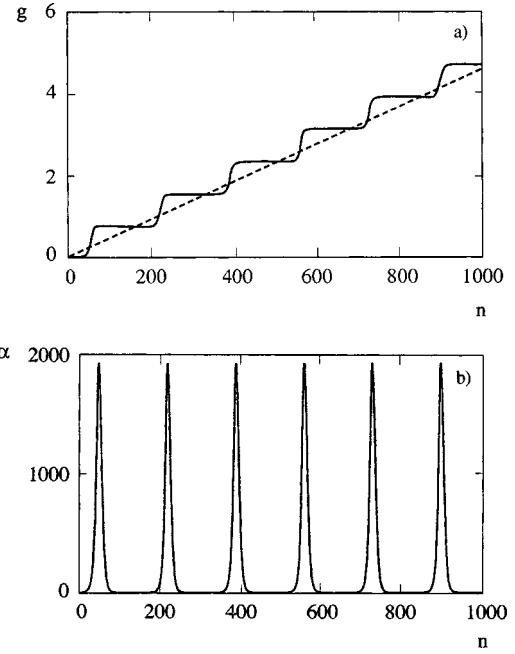


FIG. 2. (a)  $g(\cdot)$  function (continuous line) and  $2t/\tau_s$  vs time; each  $n$  step is  $2.3 \times 10^{-5}$  s; (b) growth rate parameter  $\alpha$  vs time;  $A = 9 \times 10^4$ ;  $B = 5 \times 10^4$ ;  $\tau_s = 10$  ms.

$$\frac{d}{dt} \alpha = \left[ \frac{A}{(1 + \sigma_i^2 + \sigma^2)^{1/4}} - B(1 + \sigma_i^2 + \sigma^2)^{1/2} \right], \quad (4)$$

while the first of Eqs. (1) is left unchanged. The assumptions underlying Eqs. (4) are the following.

(i) We assume that the STI induced energy spread combines quadratically with the natural part; this ensures the modification of the first of Eqs. (3) into the first of Eqs. (4).

(ii) We assume that the TIS induced energy spread combines quadratically with the STI induced part, thus allowing the modification of the second of Eqs. (1) according to the second of Eqs. (3).

The first of Eqs. (1) is left unchanged because Eq. (3) is the result of an equilibrium condition. The interplay between STI and TIS is shown in Fig. 3, where we have compared the evolution of the  $g$  and  $\alpha$  functions with and without the TIS contribution. It is evident that the presence of the TIS term modifies the STI dynamics by providing a reduction of the slope of  $g$  and of the growth rate of the instability.

### B. FEL-TIS interplay

The rate equations describing the SR-FEL evolution have already been described in Ref. [1] and are written

$$\frac{d}{dt} x_0 = Ex_0 \left[ \frac{1}{\sqrt{1 + \sigma_1^2}} \frac{1}{1 + 1.7\mu_{\varepsilon,0}^2(1 + \sigma_1^2)^{-1} r} \right],$$

$$\frac{d}{dt} \sigma_1^2 = -\frac{2}{\tau_s} (\sigma_1^2 - x_0), \quad (5)$$

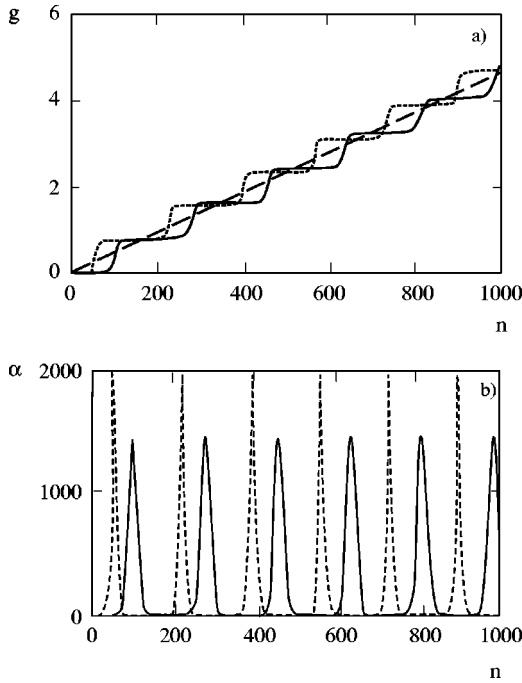


FIG. 3. Same as Fig. 1 with (continuous line) and without (dotted line) the inclusion of TIS, with  $R=0.1$ ,  $S=0.02$ .

where  $x_0$  is linked to the intracavity power density  $I$  and  $\sigma_1^2$  is the ratio of the FEL induced energy spread to the natural part. In particular, we have

$$x_0 = \mu x, \quad x = \frac{I}{I_s}, \quad \mu = \left( \frac{0.433}{N} \right)^2 \frac{\beta}{4} \frac{\tau_s}{T \sigma_{\varepsilon,n}^2}$$

$$\beta = 1.0145 \frac{\pi}{2}, \quad r = \frac{\Gamma}{0.85 g_0}, \quad \mu_{\varepsilon,0} = 4N \sigma_{\varepsilon,n}, \quad E = \frac{0.85 g_0}{T} \quad (6)$$

with  $g_0$ ,  $I_s$ , and  $\tau_s$  being the FEL small signal coefficient, the saturation intensity, and the damping time, respectively. Furthermore,  $N$  is the number of undulator periods and  $\Gamma$  the total cavity losses. The inclusion of the TIS is quite straightforward and can be done by modifying Eq. (3) and the first of Eqs. (5) as follows:

$$\sigma^2 (\sigma^2 + \sigma_1^2 + 1)^2 = R f \left( \frac{S}{(\sigma^2 + \sigma_1^2 + 1)^{3/2}} \right),$$

$$\frac{d}{dt} x_0 = E x_0 \left[ \frac{1}{\sqrt{1 + \sigma_1^2 + \sigma^2}} \frac{1}{1 + 1.7 \mu_{\varepsilon,0}^2 (1 + \sigma_1^2 + \sigma^2)} - r \right]. \quad (7)$$

The assumptions underlying Eqs. (7) are consistent with those holding for Eqs. (4); we have assumed indeed that the FEL induced energy spread combines quadratically with the natural part and that the STI energy spread contribution affects the FEL dynamics through the associated bunch lengthening and the inhomogeneous broadening contribution.

The evolution of the TIS contribution when the FEL is operating is provided in Fig. 4 and it is important to empha-

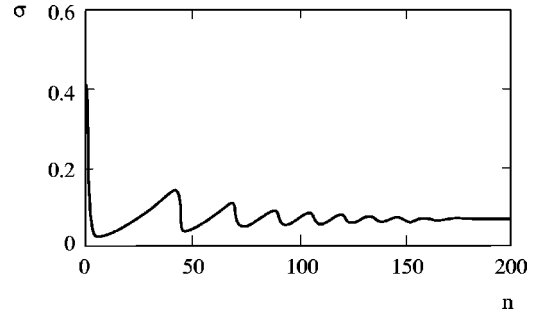


FIG. 4. TIS induced energy spread with FEL contribution:  $R=0.1$ ,  $S=0.01$ ,  $r=0.5$ ,  $E=10^5$ , and  $\tau_s=10$  ms.

size that once the FEL is on the TIS contribution is strongly reduced.

### C. FEL-STI interplay

This aspect of the problem has already been discussed in Ref. [1] and references therein. According to these papers Eqs. (1) and (5) are merged and the second of Eqs. (5) and (1) is replaced by  $\sigma_1^2 = \sigma_i^2 = \bar{\sigma}^2$ :

$$\frac{d}{dt} \bar{\sigma}^2 = \alpha \bar{\sigma}^2 - \frac{2}{\tau_s} (\bar{\sigma}^2 - x_0). \quad (8)$$

The hypothesis underlying this modelization amounts to the assumption that STI and FEL are mechanisms contributing to the generation of the same energy spread, as implicit in the loop structure of Fig. 1. The FEL-STI mutual feedback is shown in Fig. 5, where it is shown that, when the FEL is active, the slope of the function  $g$  is brought below  $2/\tau_s$  and

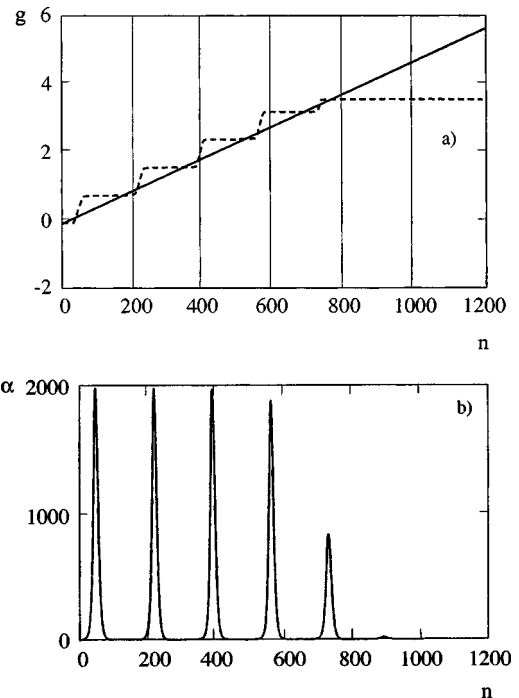


FIG. 5. Same as Fig. 2 with the inclusion of FEL with  $E=10^5$ ,  $r=0.64$ .

the amplitudes of the oscillations of the induced energy spread are reduced. The final set of equations including all the effects so far discussed can easily be written as

$$\frac{d}{dt}x_0 = Ex_0 \left[ \frac{1}{\sqrt{1+\sigma^2+\bar{\sigma}^2}} \frac{1}{1+1.7\mu_{\varepsilon,0}^2(1+\sigma^2+\bar{\sigma}^2)} - r \right],$$

$$\frac{d}{dt}\bar{\sigma}^2 = \alpha\bar{\sigma}^2 - \frac{2}{\tau_s}(\bar{\sigma}^2 - x_0), \quad (9)$$

$$\frac{d}{dt}\alpha = \left[ \frac{A}{(1+\sigma^2+\bar{\sigma}^2)^{1/4}} - B(1+\sigma^2+\bar{\sigma}^2)^{1/2} \right].$$

The model equations given in (9) are the mathematical counterpart of the loop structure of Fig. 1 and show that the modelization is flexible enough to include a significant number of physical contributions. In the forthcoming sections we will show how the model can be further developed to include contributions allowing the understanding of the effect associated with the beam lifetime.

### III. STORAGE RING FEL, NONZERO UNDULATOR DISPERSION, AND SATURATION

As already remarked, saturation in a storage ring based free-electron laser is essentially due to the turn by turn induced energy spread and to the concurrent gain reductions associated with bunch lengthening and inhomogeneous broadening. Within such a context, if we do not consider the effect of the electron-beam instabilities, the efficiency of a SR-FEL device is a function of the number of undulator periods, which relates the laser power to the synchrotron power lost in one machine turn,  $P_s$ , according to

$$P = \frac{\chi}{4N} P_s,$$

where  $\chi$  is the efficiency function depending on cavity losses, natural energy spread, and so on. The dynamics can be complicated by other effects, contributing to the saturation. One of these may be due to a nonzero dispersion function in the undulator. In this case, a further source of gain reduction arises as a contribution due to an increase of the electron-beam transverse section and thus to a poor overlapping between laser and optical beams. In this section we address this specific problem, namely, the contribution of a nonzero dispersion function inside the undulator due to the SR-FEL efficiency function.

Furthermore we will show that the FEL interaction may provide an increase of the Touscheck lifetime [4] due to the laser heating induced increase of the electron-beam volume. We will make a comparison between the theoretical results and recent experimental observations at Super-ACO. We will treat the inclusion of a nonzero dispersion inside the undulator by means of a simple extension of the previously discussed equations. We take into account the following steps.

(a) In the presence of a nonzero dispersion the beam section is provided by

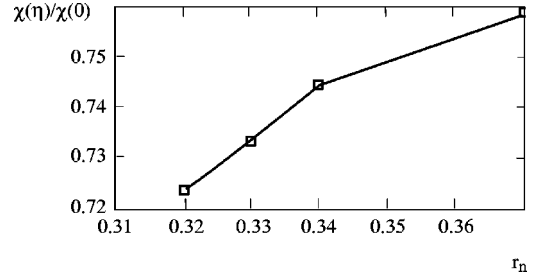


FIG. 6.  $\chi(\eta)/\chi(0)$  vs  $r$  using the experimental input values of Table I.

$$\sigma_\rho = \sqrt{\beta_\rho \varepsilon_\rho + (\eta_\rho \sigma_\varepsilon)^2}, \quad \rho = x, y, \quad (10)$$

with  $\beta_\rho$ ,  $\eta_\rho$ ,  $\varepsilon_\rho$ , and  $\sigma_\varepsilon$  being the beam envelope Twiss parameter, the dispersion function, the emittance, and the energy spread, respectively.

(b) The FEL gain is inversely proportional to

$$\Sigma = \pi \sqrt{\left(2\sigma_x^2 + \frac{w_x^2}{2}\right) \left(2\sigma_y^2 + \frac{w_y^2}{2}\right)}, \quad (11)$$

where  $w_\rho$  is the optical beam waist.

(c) We assume that only  $\eta_x \neq 0$ .

Then we can rewrite the model equation describing the SR-FEL saturation dynamics as

$$\frac{d}{dt}x_0 = Ex_0 \left[ \frac{1}{\sqrt{1+\bar{\sigma}^2}} \frac{1}{[1+1.7\mu_{\varepsilon,0}^2(1+\bar{\sigma}^2)]F(\bar{\sigma}, \eta)} - r \right] \quad (12)$$

where

$$F(\bar{\sigma}, \eta) = \frac{1}{\sqrt{1+A(1+\bar{\sigma}^2)}} \frac{1}{\sqrt{1+1/[1+A(1+\bar{\sigma}^2)]}},$$

$$A = \left( \frac{\sigma_{\varepsilon,n} \eta_x}{\sqrt{\varepsilon_x \beta_x}} \right)^2, \quad a = \frac{w_x^2}{2\beta_x \varepsilon_x}. \quad (13)$$

The contribution to the dynamics due to the nonzero dispersion function is provided by the function  $F(\bar{\sigma}, \eta)$ . Since we are interested to the efficiency of the device, we will consider the steady state solution of Eq. (3), which provides the dimensionless intracavity steady state power as a solution of the nonlinear algebraic equation

$$\frac{1}{\sqrt{1+x_e}} \frac{F(0, \eta)}{[1+1.7\mu_{\varepsilon,n}^2(0)(1+x_e)]} \frac{1}{\sqrt{1+A(1+x_e)}} \times \frac{1}{\sqrt{1+1/[1+A(1+x_e)]}} = r,$$

$$F(0, \eta) = \sqrt{1+A+a}. \quad (14)$$

According to Ref. [1] the output laser power is linked to the synchrotron radiation power by

TABLE I. Experimental values of the parameters appearing in Eq. (14).

$r_1=0.32$	$\sigma_{\varepsilon,n}^1=8.3\times 10^{-4}$
$r_2=0.33$	$\sigma_{\varepsilon,n}^2=8.6\times 10^{-4}$
$r_3=0.34$	$\sigma_{\varepsilon,n}^3=9.1\times 10^{-4}$
$r_4=0.37$	$\sigma_{\varepsilon,n}^4=9.3\times 10^{-4}$
$A_1=6.16$	$a_{1,\dots,4}=16.85$
$A_2=6.61$	
$A_3=7.24$	
$A_4=7.73$	

$$I_{\text{out}} \approx \frac{\chi}{4N} P_s, \quad (15)$$

where the efficiency function  $\chi$  is given by

$$\chi = 1.422 r x_e \mu_{\varepsilon,n}^2. \quad (16)$$

In Fig. 6 we show the relevance of the contribution of a nonzero dispersion to the saturation function. It is evident that this effect provides a reduction of the out-coupling efficiency. We have reported the ratio  $\chi(\eta)/\chi(0)$  using as input the experimental values (see Table I) and find a reduction of the efficiency of the order of 20–30% in agreement with the experimental observations. According to the above analysis it is evident that the presence of a nonzero dispersion in the undulator may provide a reduction of the laser power with respect to the case in which  $\eta$  is zero.

Let us discuss the effect of the FEL on the Touscheck electron-beam lifetime, which for a flat beam is written (MKSA units) [4]

$$\begin{aligned} \tau &= 8\pi \frac{\gamma^2 \sigma_x \sigma_y \sigma_z}{N r_0^2 c \lambda^3 D(\varepsilon)}, \quad \lambda = \frac{\gamma m_0 c}{\varepsilon_{rf}}, \\ \varepsilon &= \frac{2}{\lambda^2 \gamma^2} \left( \frac{\beta_x^2}{4\sigma_x^2} - \frac{B_1^2}{4A_1} \right), \\ D(\varepsilon) &= \sqrt{\varepsilon} \left[ -\frac{3}{2} e^{-\varepsilon} + \frac{\varepsilon}{2} \int_{\varepsilon}^{\infty} \frac{\ln u}{u e^u} du + \frac{1}{2} (3\varepsilon + \varepsilon \ln \varepsilon) \right. \\ &\quad \left. + 2 \int_{\varepsilon}^{\infty} \frac{e^{-u}}{u} du \right], \quad (17) \end{aligned}$$

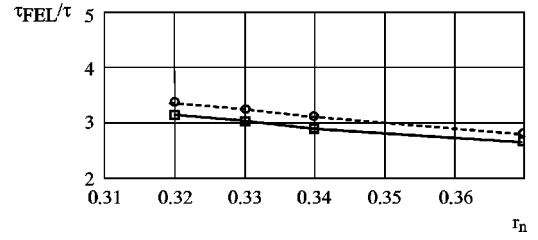


FIG. 7.  $\tau_{\text{FEL}}/\tau$  vs  $r$ , as in Fig. 6; experiment (continuous line); theory (dotted line).

where  $r_0$  is the electron classical radius,  $\varepsilon_{rf}$  the radio-frequency acceptance,  $\gamma$  the energy relativistic factor,  $N$  the number of particles in the bunch, and

$$\begin{aligned} A_1 &= \frac{1}{4\sigma_\varepsilon^2} + \frac{1}{4\sigma_x^2} \left[ \eta^2 + \frac{1}{4} (\beta_x \eta' - \beta'_x \eta)^2 \right], \\ B_1 &= \frac{\beta_x}{4\sigma_x^2} (\beta_x \eta' - \beta'_x \eta). \quad (18) \end{aligned}$$

$\sigma$  denotes the rms beam size (where the primes denote derivative with respect to the longitudinal coordinate  $s$ ). According to the previous discussion the increase of the lifetime may come through increase of the bunch volume and through the  $\eta$  function.

An idea of how the Touscheck lifetime may be modified by the FEL is offered by Fig. 7, where we have plotted  $\xi = \tau_{\text{FEL}}/\tau$  and make a comparison with the experimental results. It is evident that, when the FEL is on, we may have a significant increase of the Touscheck lifetime and the theoretical predictions are in close agreement with the observed increasing lifetime.

The fact that the theoretical analysis overestimates the experimental values can be simply explained by noting that we have assumed that the transverse section increase occurs over the whole machine and not in the interaction region only.

## ACKNOWLEDGMENTS

This work has been performed under European network Contracts No. ERBF MRXCT980245 and EUFELE HPRI-CT-2001-50025.

- [1] R. Bartolini *et al.*, Phys. Rev. Lett. **87**, 134801 (2001).  
 [2] G. Dattoli *et al.*, Phys. Rev. E **58**, 6570 (1998).  
 [3] R. Roux and M. Billardon, Nuovo Cimento Soc. Ital. Fis., A **112**, 513 (1999).  
 [4] J. Le Duff, in *Proceedings of the CAS CERN Accelerator School 95-06* (CERN, Geneva, 1995), Vol. II, p. 573.  
 [5] M. Hosaka *et al.*, Nucl. Instrum. Methods Phys. Res. A **407**, 234 (1998).  
 [6] J. M. J. Madey, Nuovo Cimento Soc. Ital. Fis., B **50**, 64

- (1979).  
 [7] M. Sands, SLAC Report No. 121, 1970 (unpublished).  
 [8] C. Bruni *et al.*, Nucl. Instrum. Methods Phys. Res. A **483**, 167 (2001).  
 [9] R. Baartman and M. D'Yachkov, in *Proceedings of Particle Accelerator Conference 1995* (CERN, Geneva, 1995), p. 3119.  
 [10] M. Migliorati *et al.*, Nucl. Instrum. Methods Phys. Res. A **437**, 134 (1999).  
 [11] G. Dattoli *et al.* (unpublished).